~~RESTRICTED~~

RM No. A7D10

RESEARCH MEMORANDUM

THE DEVELOPMENT OF JET-ENGINE NACELLES FOR A HIGH-SPEED BOMBER DESIGN

By

Robert E. Dannenberg

Ames Aeronautical Laboratory
Moffett Field, Calif.

~~RESTRICTED DOCUMENT~~

NATIONAL ADVISORY COMMITTEE FOR AERONAUTICS

WASHINGTON

August 29, 1947

~~RESTRICTED~~

NACA RM No. A7D10 ~~RESTRICTED~~

NATIONAL ADVISORY COMMITTEE FOR AERONAUTICS

RESEARCH MEMORANDUM

THE DEVELOPMENT OF JET-ENGINE NACELLES FOR A HIGH-SPEED BOMBER DESIGN

By Robert E. Dannenberg

SUMMARY

The results of an experimental investigation made for the purpose of developing suitable jet-engine nacelle designs for a high-speed medium bomber are presented. Two types of nacelles were investigated, the first enclosing two 4000-pound-thrust jet engines and a 65-inch-diameter landing wheel and the second enclosing a single 4000-pound-thrust jet engine. Both types of nacelles were tested in positions underslung beneath the wing and centrally located on the wing.

This report summarizes the investigation which was performed at low speed for the purpose of developing entrance and body shapes of suitable form. Included are results from the high-speed portion of the investigation on the characteristics of an underslung nacelle.

The nacelles developed show desirable aerodynamic characteristics. The pressure recovery of the internal flow at the face of the compressor is found to be greater than 90 percent of the free-stream dynamic pressure for all flight conditions tested. The drag of all nacelles compares very favorably with similar bodies used for housing conventional air-cooled engines, the average drag coefficient based on frontal area being approximately 0.050. Locating the nacelle in an underslung position beneath the wing resulted in an expected shift of the angle-of-zero lift due to the adverse effects on the span load distribution. Negligible adverse interference effects on the maximum lift and pitching-moment characteristics were experienced. The critical-compressibility speed for the combination of the wing and each nacelle is equal to or above that of the plain wing at inlet-velocity ratios

greater than 0.6.

INTRODUCTION

In order to utilize most efficiently the research facilities of the laboratories of the National Advisory Committee for Aeronautics, the Air Technical Service Command of the United States Army Air Forces in announcing a new design competition for a medium jet-propelled bombardment airplane conferred with members of the staff of the NACA to formulate a research program which would adequately cover all research needs associated with the bomber design competition. The various research programs needed to provide design information were formulated in conferences at Wright Field. This report presents a summary of the research concerning the development of satisfactory jet-engine nacelles that was undertaken at the Ames 7- by 10-foot and 16-foot wind tunnels by W. F. Davis, G. B. McCullough, G. E. Allison, J. R. Pengal, and the author.

The nacelles investigated were specified as follows:

A. A nacelle underslung beneath the wing housing two 4000-pound-thrust axial-flow jet engines and one 65-inch-diameter landing wheel

B. A nacelle centrally located on the wing enclosing two 4000-pound-thrust axial-flow jet engines and a 65-inch-diameter landing wheel

C. A nacelle underslung beneath the wing enclosing one 4000-pound-thrust axial-flow jet engine

D. A nacelle centrally located on the wing housing one 4000-pound-thrust axial-flow jet engine

Views of these nacelles are shown in figure 1.

In developing the nacelles the following requirements were outlined as being necessary for a satisfactory design:

1. The arrangement of jet engines and wheels to give satisfactory aerodynamic characteristics without introducing undesirable structural, maintenance, or accessibility problems

2. The attainment of as high critical-compressibility speed for the wing-nacelle combination as for the isolated wing of the airplane

3. The attainment of low external drag throughout the speed range

4. The attainment of very low total-pressure losses in the internal-flow system up to the face of the jet-engine compressor and a uniform distribution of velocity over the face of the jet-engine compressor at all operating conditions

5. Minimum interference effects of the nacelles on the lift and moment characteristics

SYMBOLS

C_L	lift coefficient (L/qS)
L	lift force, pounds
S	wing-panel area, square feet
C_D	total drag coefficient (D/qS)
D	total drag force (sum of drag of wing panel, nacelle, and intake air), pounds
C_{D_F}	external drag coefficient of nacelle (D_F/qF)
D_F	external drag force of nacelle (difference between total drag and sum of wing-panel and intake-air drag forces), pounds
F	frontal area of nacelle, square feet
q	free-stream dynamic pressure ($\frac{1}{2}\rho V_o^2$), pounds per square foot
V_o	free-stream velocity, feet per second
ρ	mass density, slugs per cubic foot

α	angle of attack based on wing chord line, degrees
c	chord of wing panel at tunnel center line, feet
$C_{m_{c/4}}$	pitching-moment coefficient about quarter-chord line of wing panel $(M_{c/4}/qcS)$
$M_{c/4}$	pitching moment about the quarter-chord line, pound-feet
M_{cr}	critical Mach number
V_i	velocity of air at duct entrance, feet per second
V_i/V_o	inlet-velocity ratio
P	pressure coefficient $[(p_l-p)/q]$
p	free-stream static pressure, pounds per square foot
p_l	local static pressure, pounds per square foot

DESCRIPTION OF MODEL AND APPARATUS

The wing panel with the various nacelles was mounted vertically in the Ames 7- by 10-foot wind tunnel so that the span extended across the 7-foot dimension of the test section as indicated in figure 2. The model wing panel represented a scaled portion of the span of a typical high-speed bomber aircraft with an untwisted wing of aspect ratio 9.0 and a taper ratio of 2.5 to 1.0. Figure 3 shows a sketch of this airplane with the portion of the span used for the model tests designated. An NACA 65$_1$-210 airfoil section was used. The wing panel area was 22.802 square feet while the chord at the tunnel center line was 3.359 feet.

A model scale of 0.2166 was used which corresponded to an airplane span of 116 feet. The center lines of the nacelles were located 13.35 percent of the wing span outboard from the plane of symmetry of the full-scale wing. The model was equipped with both 25-percent-chord slotted flaps and 30-percent-chord split flaps.

All nacelles in the series were mounted in the same relative position on the wing. Air was drawn through the inlet ducts of each model by an aircraft-type supercharger that was located outside the test chamber. The air flowed through the inlet ducts into a plenum chamber in the center of each nacelle as shown in figure 2; from there it was drawn through the hollow spar of the wing, then through a mercury seal that isolated the ducting from the scale system, and finally into the supercharger.

The quantity of air flowing through the internal-duct system was measured by the pressure drop across a calibrated orifice and controlled by a throttle. The measurements of the internal-duct losses and the velocity distribution at the face of each compressor were measured by a rake consisting of 36 total-pressure and 4 static-pressure tubes connected to an integrating manometer. The pressure distribution over critical sections of the nacelle was measured by flush-type orifices that were connected to multiple-tube manometers and photographically recorded.

Design of Nacelle

The design of each nacelle was based primarily on the location of the internal members (jet engine and landing wheel) with respect to the wing. The jet engines of the two-unit nacelles were placed well forward on the wing to aid in providing proper balance to the airplane. Their forward position was limited, however, for the tail pipes could not be of such length as to cause excessive losses in engine thrust. As references 1 and 2 showed the advantage of a cusped-type outlet, the landing wheel was retracted into a forward portion of the nacelle to allow the afterbody to taper more gradually and the center of gravity of the landing gear to be forward during normal flight. To obtain the cusped-type afterbody shape it was necessary to curve the tail pipes slightly to form contiguous tail-pipe exits.

In designing the external shape of the nacelles, the frontal and surface areas were kept as small as possible. These areas were determined to a certain extent by the pressure distribution that was required. The forebody of each nacelle was designed to produce a distribution of velocity along the nacelle and over the lips which would give no localized velocity peaks. Based on the results of

references 1 and 2, a lip shape was selected with a lip radius of approximately 0.005 times nacelle chord and cambered as indicated from the references. Contracting the lines of the internal duct slightly aft of the lip prevented stalling of the flow from the inner surface at high angles of attack and permitted very high pressure recoveries for all operating conditions. The elliptical-type nose entrance was used on the two-unit nacelles as it made possible a more uniform distribution of camber and thickness about the periphery of the nose inlet than was possible with separate circular or rectangular entrances.

In the vicinity of the wing, the longitudinal curvature of each nacelle faired into the main body of constant cross-section. The general body lines were selected to give constant cross-section area for the central section of each nacelle to minimize the incremental velocities over the nacelle in the region of the wing. The shape of the afterbody was designed to avoid severe adverse pressure gradients and tapered down to a cusped outlet (reference 1).

The inlet area of each duct entrance was designed for a high-speed inlet-velocity ratio of 0.6 which would meet the air-flow requirement of each engine at a true airspeed of 550 miles per hour at an altitude of 40,000 feet. This value of the inlet-velocity ratio was selected (reference 2) because it was high enough to prevent the formation of low-pressure regions on the external surfaces of the duct lips and still permit a high internal pressure recovery. The twin-unit intake ducts separate from a common entry at the nose of the nacelle and expand at a constant rate in an expansion ratio of 1:1.2 from a semielliptical entrance shape to a circular section at the compressor inlet. The single-engine nacelles have the same expansion ratio with a circular inlet shape. The expansion is gradual and there are no sharp bends in the ducts so that separation of the internal flow is avoided. The detail of the internal duct systems is shown in the cutaway drawings on figures 1 and 2.

The body lines of each nacelle were sketched about the wing and internal members. In order to better visualize the proposed nacelle shape, a small wooden model of the wing, jet engines, and landing wheel was assembled to scale and covered with modeling clay. The clay was faired to the proposed body

lines to permit a visual examination of the nacelle shape. The small models were of particular aid in developing the fairing from the wing trailing edge to the nacelle afterbody. After the nacelle lines were developed with the designed lip radius, cambered forebody, straight center section and cusped afterbody, the five control lines were matched with second-degree curves by the proper selection of the control points as explained in the appendix. The control line drawings for the nacelles are shown in figures 4 to 7.

TESTS

All the data have been corrected for fluid compressibility and for tunnel-wall interference on the wing panel. The tare forces resulting from the skin-friction drag of the wind-tunnel stream flowing across the end plates of the model and from leakage about the end plates have not been measured and are included in the force-test data because they are small and would have no effect upon the incremental forces caused by the addition of a nacelle to the wing. The test results are presented for a Mach number of 0.14 and a Reynolds number of approximately 3,400,000 based upon the chord of the wing panel at the tunnel center line, 40.310 inches. All test results were obtained with a tail cone installed as shown in figure 2.

The external drag of each nacelle was obtained by subtracting the drag of the wing panel and the drag of the internal flow system from the total drag as measured by the wind-tunnel scale system. The internal drag was computed from the measurements of the quantity of air flowing through the duct system by the method of reference 1. It may be seen readily that as the wing and internal drag forces are large in comparison with the total drag force, any inaccuracy in measurement would appear as a large proportion of the external drag force. In order to reduce this error to a minimum, particular care was taken in obtaining all drag measurements; and the accuracy of the external nacelle drag, based upon its frontal area, was within ±5 percent.

The constriction effects resulting from the large size of the two-unit nacelles relative to the tunnel size were

estimated from reference 3 to have resulted in about a 3-percent error in the dynamic pressure. The effect of air induction into the nacelle nose also caused an error in the dynamic pressure which was of approximately the same magnitude, but of opposite sign. As these two corrections tended to compensate each other, no correction was made for either.

RESULTS AND DISCUSSION

This report summarizes the results of tests encountered in the design of nacelles for installation on a thin, low-drag high-critical-speed wing. In applying the test results to the design of a nacelle, the limitations of the wind tunnel must be taken into account. The effect of three-dimensional flow upon the entire wing will change the incremental values, particularly in the high-lift attitudes where the stalling characteristics of the wing panel will be different.

Lift Characteristics

The addition of the underslung nacelles to the wing panel, flaps retracted, resulted in an increase in the angle of zero lift and consequent loss in lift at low angles of attack; whereas the centrally located nacelles showed no appreciable change. However, the slope of the lift curve increased slightly for all nacelles. The change in the lift-curve characteristics, shown in figure 8, is also tabulated in table I. The increment in maximum lift due to the slotted flaps was reduced by the addition of the nacelles partly because of the decrease in flap span (twin-unit nacelles) and also because of the interference of the nacelles upon the circulation about the wing. On a full-scale airplane, the airplane loss in lift would be reduced to about two-thirds of that shown in the wind-tunnel tests as the wing panel represents 64.6 percent of the semispan wing area. The lift characteristics were found to be independent of the inlet-velocity ratio.

The slight change in the lift characteristics of the wing, resulting from the addition of the central nacelles, indicates that the spanwise lift distribution of the wing would remain

almost unchanged, which is a desirable characteristic for aerodynamic and structural design. For the under-slung nacelle, however, the incremental velocities add only to the wing lower-surface velocities decreasing the lift over the portion of the wing affected by a nacelle. This characteristic is undesirable and should be reduced to a minimum in order to remove the irregularity in the span-wise load distribution. Modification of the wing adjacent to the nacelles to give increased camber or chord or a combination of both may be used to alleviate this condition.

To restore some of the maximum lift loss due to nacelles, slotted flap deflected, the clearance between the deflected flap and the side of the underslung nacelle was reduced to a minimum by extending the flap, resulting in the increased lift shown in figure 9. The central nacelle maximum lift losses were reduced to negligible amounts by the addition of a simple split flap (fig. 9) to bridge th cutout in the slotted flap and shaped to fit the contour of the nacelle when in the retracted position.

The lift characteristics of the plain wing and nacelle A with 30-percent-chord split flaps are also shown in figure 9. Reducing the clearance between the nacelle and the deflected flap to a minimum increased the maximum lift.

Drag Characteristics

The total drag polars of the various wing-nacelle combinations are shown in figure 10 for zero inlet-velocity ratio. The drag characteristics, flaps deflected, are presented in figure 11. The external-drag coefficients of the nacelles, based on the frontal areas given in table I, are shown in figure 12 for various inflow rates.

The large variation of the external drag of the under-slung nacelles with angle of attack was caused by the change in the span load distribution. As this effect is undesirable structurally and aerodynamically, it is believed that the

condition may be improved by extending the wing chord near the nacelle.

Figure 13 was cross-plotted to show the variation of nacelle drag with inlet-velocity ratio at angles of attack corresponding to that for high-speed flight and climb. In the range of normal flight velocities, the external drag of the underslung nacelles remained below that of the central nacelles. The effect of drawing air into the ducts of all nacelles was to reduce the external drag.

Pitching-Moment Characteristics

The effect of all nacelles on the plain wing pitching-moment characteristics was destabilizing as shown in figure 14. The variation in dC_m/dC_L is tabulated for all nacelles in table I. Though this effect may be minimized by reducing the length of nacelle ahead of the wing, the change may have an adverse effect on the critical-speed characteristics.

Internal Flow

The total pressure recovery at the face of the compressor for the various nacelles was found to be satisfactory, the pressure recovery being over 93 percent of the dynamic pressure and the velocity distribution varying less than ±2 percent. Both single-unit nacelles obtained 100-percent pressure recovery within the limit of accuracy of measurement as shown in table I. These low internal-flow losses were due to the very small expansion of the internal ducting. The fact that the losses remained low over a wide range of velocity ratios through the angle-of-attack range showed the use of large lip radii and shaping of the inner surface of the lower lip to be satisfactory.

It will be noted that no provision was made for bleeding air from the intake system for use in cooling the after-portion of the motor. For these nacelles it is anticipated that cooling air could be supplied by small submerged duct entrances on the sides or under-surface of the nacelle body.

Single-Unit Operation of a Two-Unit Nacelle

As long-range flight may require single-unit operation of a two-unit nacelle for maximum economy, one duct of nacelle A was closed off by means of a solid plate inserted behind the rake. All the air then passed through the other duct. The pressure recovery in this condition remained unchanged at low inflow rates and dropped off but slightly at high inlet velocities; for an inlet-velocity ratio of 1.20 the recovery was 94 percent. The lift, drag, and pitching-moment characteristics remained unchanged from that with dual operation.

Pressure Distribution and Estimated Critical Speed

The pressure distribution over the corresponding basic lines of each nacelle (upper and lower center lines and maximum half-breadth line) was found to be so similar that all were represented by a single typical curve at a given inlet-velocity ratio. The estimated critical speed characteristics for the external lips (first 10 percent of nacelle length) are shown in figures 15(a), 16(a), and 17(a), while representative pressure-distribution curves are given in figures 15(b) to 17(b) for various angles of attack. The critical Mach number characteristics have been estimated from the low-speed pressure distribution by the method of reference 4, which is applicable to two-dimensional flow only. However, the deviation from the more precise theory (reference 5) is negligible for bodies of fineness ratios of the order used for the nacelle while it is believed that the lip shapes and camber used on the nacelles are about the optimum, some decrease in lip camber may be permitted without serious effects.

The typical pressure distribution over the nacelle is presented in figures 15(c) to 17(c), while the estimated critical Mach number variation is shown in figures 15(d) to 17(d). As no severe adverse pressure gradients occurred over any nacelle forebody for the normal high-speed flight range and as the critical-compressibility speeds at inlet-velocity ratios greater than 0.6 were in general above that of the plain wing, the nacelle design was considered satisfactory.

The measured pressure distribution (figs. 18 and 19) for the wing-nacelle juncture for all nacelles was independent of inflow rate. A marked decrease in the lift-coefficient range for high critical speed compared to that for the wing was noted. Analysis of the flow around prolate spheroids showed this to be due to the fact that the juncture airfoil sections experience an angle-of-attack change appreciably greater than the geometric angle-of-attack change given the wing. This results in the early formation of pressure peaks on the nose of the juncture airfoil sections with a consequent premature rapid decrease in the estimated critical speed.

In order to eliminate this pressure peak the nacelle-wing juncture of nacelle A was filleted at the leading edge of the juncture section so that, in plan form, the juncture section becomes of greater chord as the nacelle is approached. Figure 18 shows drawings of the juncture in its basic and modified form. The effect of the fillet on the pressure distribution of the juncture is also shown. It should be stated that nose pressure peaks in the juncture are quite localized and are in a generally favorable pressure gradient. The effect of this local peak on the drag of the wing-nacelle combination cannot be estimated.

The addition of the centrally located nacelles to the wing resulted in an appreciable increase in the minimum-pressure peak of the wing at 50-percent wing chord. This reduced the critical speed of the combination below that of the wing even at the high-speed lift coefficients. The use of long-chord fillet airfoil sections reduced the adverse influence of the nacelle on this pressure peak (fig. 19).

High-Speed Tests

The twin-unit nacelles were investigated in the Ames 16-foot high-speed wind tunnel. Some of the high-speed characteristics of nacelle A are presented in figure 20 in order to show a brief comparison between the low-speed estimated critical Mach number characteristics and the actual high-speed results. It may be noted that the presence of the nacelles had no appreciable effect on the Mach number for drag divergence compared to the basic wing-fuselage combination. The only appreciable effect of the

nacelles is to steepen the rise of the drag curve after the Mach number for divergence is reached. Nacelle B exhibited high-speed characteristics similar to those of nacelle A.

CONCLUSIONS

The results of tests of the specific nacelle designs for the high-speed bomber competition show the following:

1. Low external drag (C_{D_F}~0.050 based on frontal area) for all nacelles, a value comparable with the best radial-engine nacelles

2. Desirable critical-speed characteristics for the two-unit nacelles with negligible effect on the Mach number for drag divergence but with some steepening of the drag coefficient rise after the Mach number for divergence is reached

3. Negligible effects on lift characteristics of the wing for the centrally located nacelles and an undesirable but expected shift of the angle of zero lift for the underslung nacelles

4. Small destabilizing pitching-moment effects for all nacelles

5. Excellent internal-flow characteristics

6. Critical-compressibility speed of the wing and each nacelle equal to or better than the 10-percent-thick wing at inlet-velocity ratios greater than 0.6

Ames Aeronautical Laboratory,
National Advisory Committee for Aeronautics,
Moffett Field, Calif.

APPENDIX

LOFTING PROCEDURE

The control lines used in the construction of each nacelle shown in figures 4 to 7 were developed by use of the methods of conic lofting described in reference 6. The use of conic development was advantageous as it allowed a rapid, accurate duplication of the original design to any scale and assured true fairness of all of the surfaces as the rate of change of curvature at any position on the body was continuous.

In designing the various nacelles, three basic or control lines, the upper and lower center lines (elevation) and the maximum half-breadth line (plan) were first free-faired to fit about the jet motor and internal-flow system with the designed lip radius, required camber in the forebody, straight center section, and cusped afterbody. Upper and lower shoulder development lines faired in diagonal planes determined the roundness of the longitudinal sections and were selected from inspection of the forebody and afterbody plan views. All five development lines were then matched as closely as possible with second-degree curves by proper selection of the control points. The method used in determining a conic curve from control points is shown in figure 21, where, for example, by translation of the axes, point O would correspond to the start of the straight center section of a nacelle; point B and tangent line AB would be determined by the intersection of the curve and the lip leading-edge circle; and point D would be a required point on the curve. Thus, by selecting the origin of the axes system, as shown in figure 21(a), the solution for each of the required curves was found directly by evolution of the five constants. The basic dimensions of the control lines have been selected to even hundredths of an inch, while the dimensions that have been derived from them were computed to ten-thousandths of an inch.

The upper and lower center lines (elevation), the maximum half-breadth line (plan), and the upper and lower shoulder lines (body plan) completely define each nacelle shape, as all nacelles were designed symmetrically about the center line plane. By dividing the half sections of each nacelle into two quadrants, it was readily seen that the upper quadrant was determined by the upper center line, the upper shoulder line

and the maximum half-breadth line. The lower quadrant was determined by the maximum half-breadth line, lower shoulder line, and lower center line. Thus, any intermediate nacelle station contour was developed by the graphical construction method shown in figure 21(b) where the points O, D, and B represent the intersection of the station plane with the upper or lower quadrants.

REFERENCES

1. Becker, John V.: Wind-Tunnel Tests of Air Inlet and Outlet Openings on a Streamline Body. NACA ARR, Nov. 1940.

2. Allen, H. Julian, Frick, Charles W., and Erickson, Myles D.: An Experimental Investigation of Several Low-Drag Wing-Nacelle Combinations with Internal Air Flow. NACA ACR No. 5A15, 1945.

3. Robinson, Russell G., and Wright, Ray H.: Estimation of Critical Speeds of Airfoils and Streamline Bodies. NACA ACR, Mar. 1940.

4. von Kármán, Th.: Compressibility Effects in Aerodynamics. Jour. Aero. Sci., vol. 8, No. 9, July 1941, pp. 337-356.

5. Herriot, John G.: The Linear Perturbation Theory of Axially Symmetric Compressible Flow, with Application to the Effect of Compressibility on the Pressure Coefficient at the Surface of a Body of Revolution. NACA RRM No. A6H19, 1946.

6. Liming, Roy A.: Practical Analytic Geometry with Applications to Aircraft. The MacMillan Company, 1944.

TABLE I.- SUMMARY OF NACELLE CHARACTERISTICS

Model	Plain Wing	A	B	C	D
Type	-----	Underslung	Central	Underslung	Central
Number of jet engines	-----	2	2	1	1
Number of wheels	-----	1	1	0	0
Frontal area, sq ft	-----	2.153	2.039	.865	.885
Total inlet area, sq ft	-----	.259	.259	.129	.108
Jet motor area, sq ft	-----	.145	.145	.145	.145
Nacelle incidence, deg	-----	-1.5	-1.5	-1.5	0
Nacelle length, in.	-----	81.45	77.20	71.22	64.82
Maximum lift, $C_{L_{max}}$	0.985	1.000	.980	1.025	.990
Angle zero lift, deg	-1.1	.1	-.9	-.4	-1.1
$dC_L/d\alpha$	1.015	1.110	1.155	1.125	1.055
dC_M/dC_L	.010	.065	.085	.016	.019
C_{DF}, nacelle drag based on frontal area, $V_i/V_o = 0.8$; $\alpha = 0^\circ$	-----	.047	.044	.068	.054
$\alpha = 1^\circ$	-----	.042	.044	.058	.054
$\alpha = 4^\circ$	-----	.024	.035	.035	.044
Pressure recovery for $V_o = 0$, based on entrance dynamic pressure	-----	.94	.95	.98	.97
Dynamic Pressure Recovery; $V_i/V_o = 0.4$	-----	1.00	.99	1.00	1.00
.8	-----	.99	.98	1.00	1.00
1.2	-----	.96	.93	1.00	1.00
1.6	-----	.91	.84	1.00	1.00

NATIONAL ADVISORY
COMMITTEE FOR AERONAUTICS

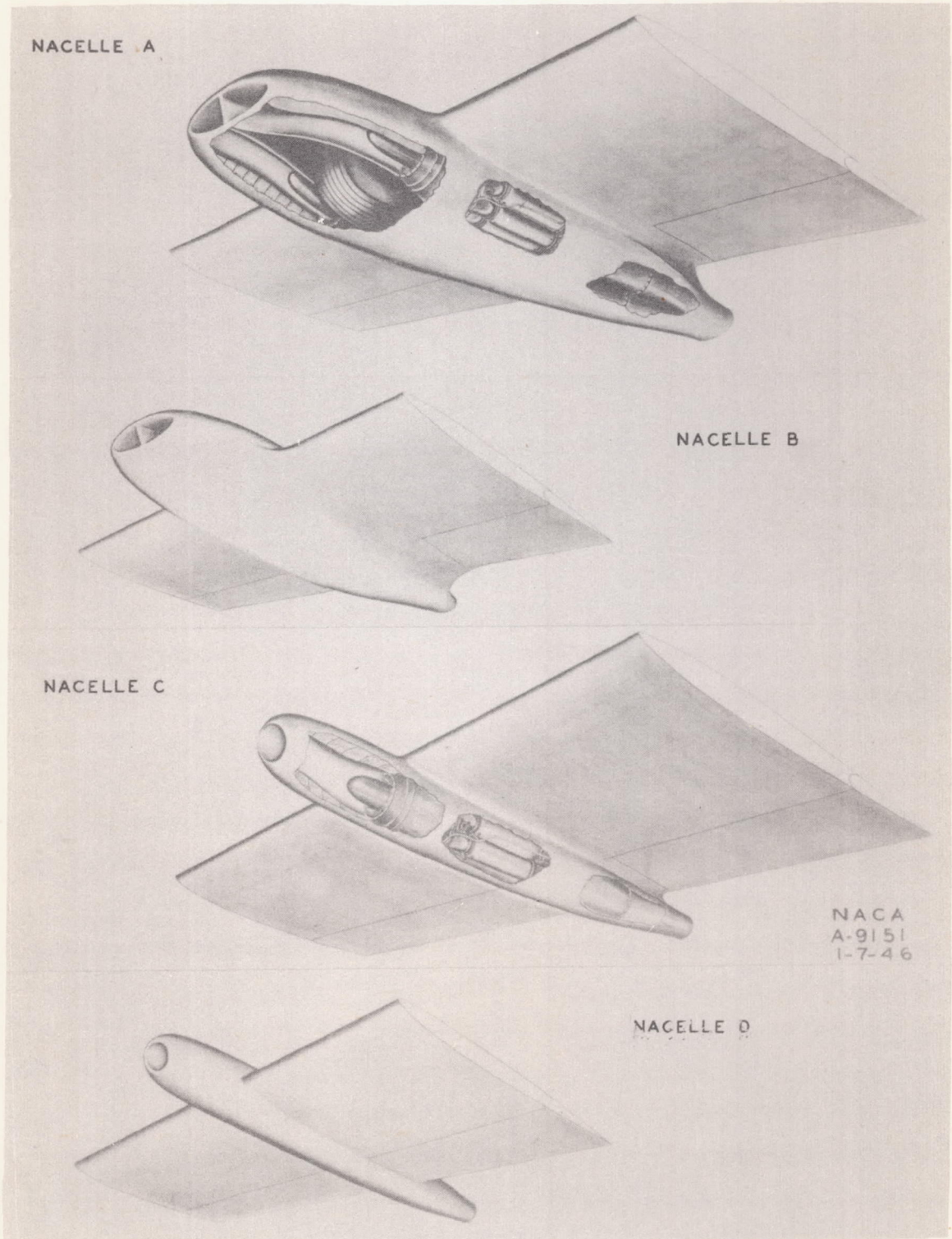

Figure 1.- Sketch of the nacelles mounted on the wing panel.

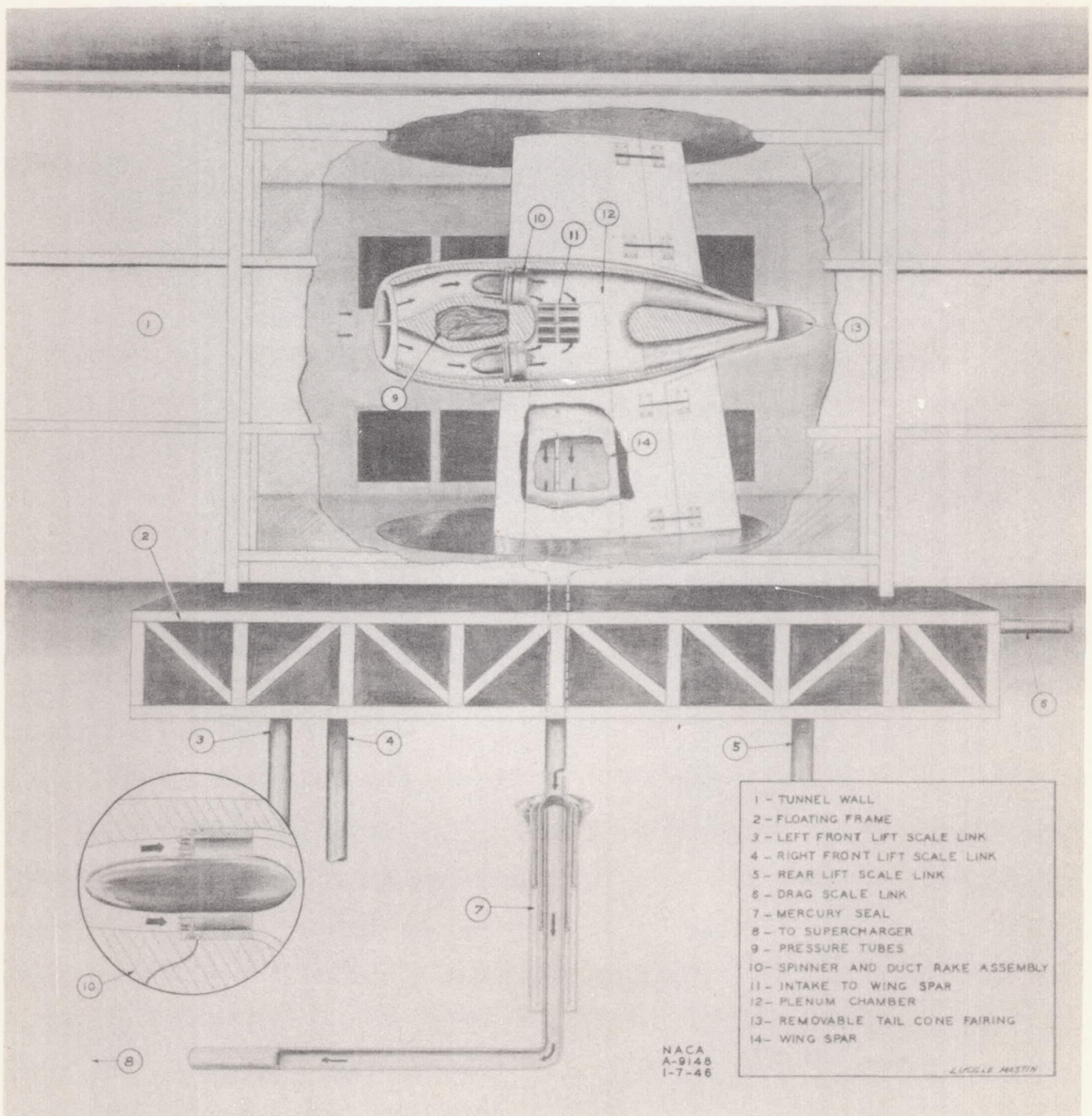

Figure 2.- Model installation in test section.

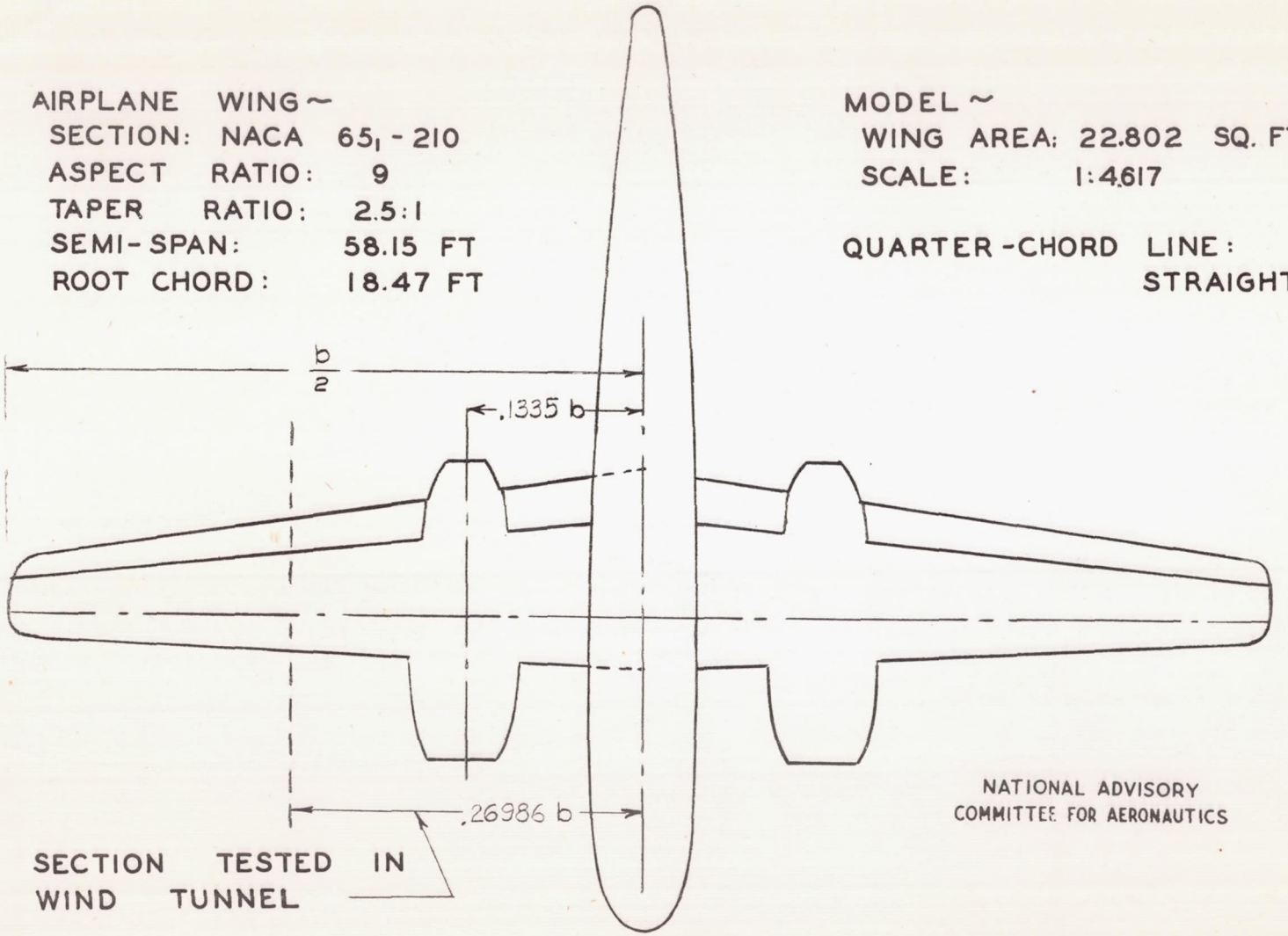

FIGURE 3.- PLAN OF HIGH-SPEED AIRPLANE SHOWING SECTION USED IN TEST.

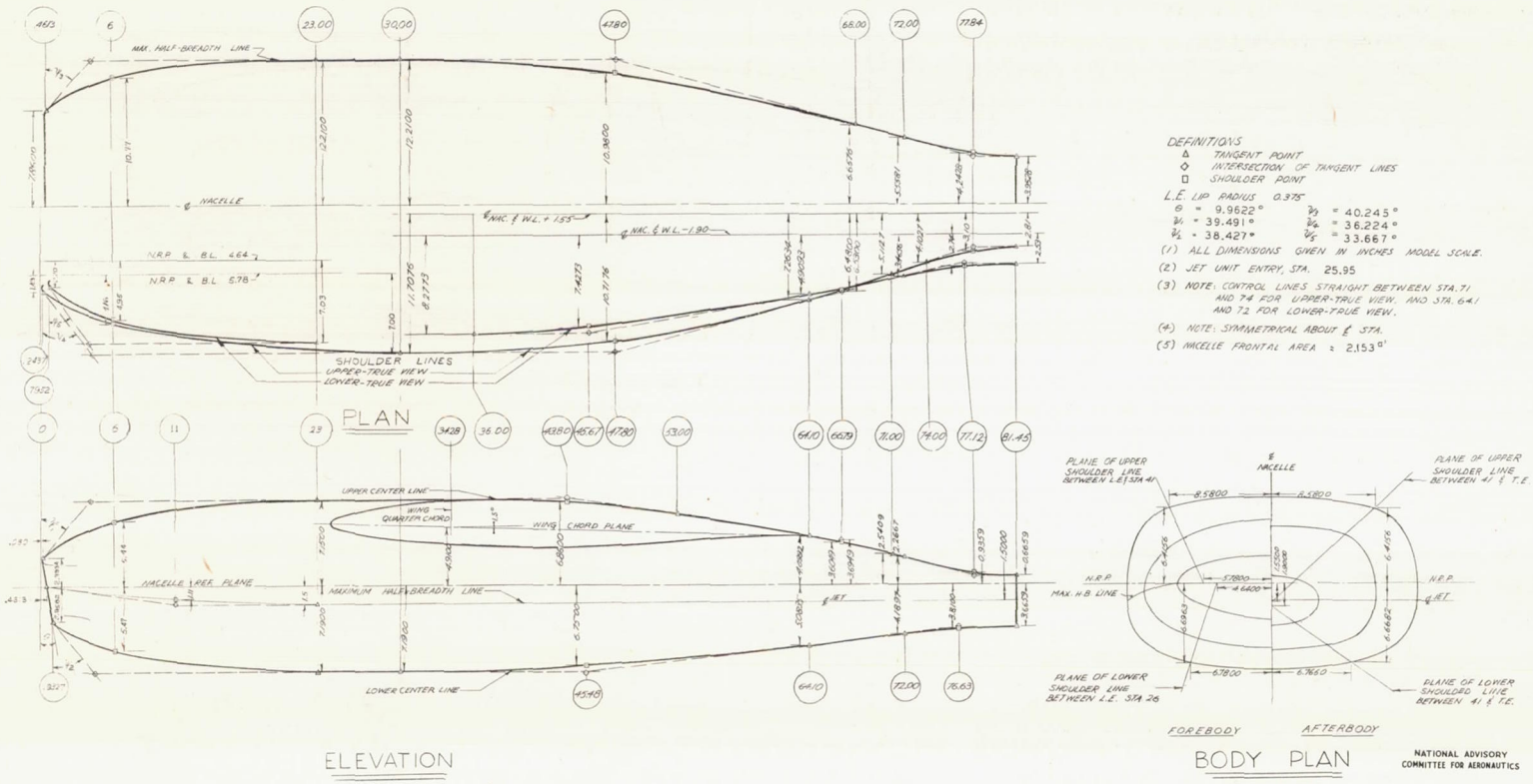

FIGURE 4.- CONTROL LINES FOR NACELLE A.

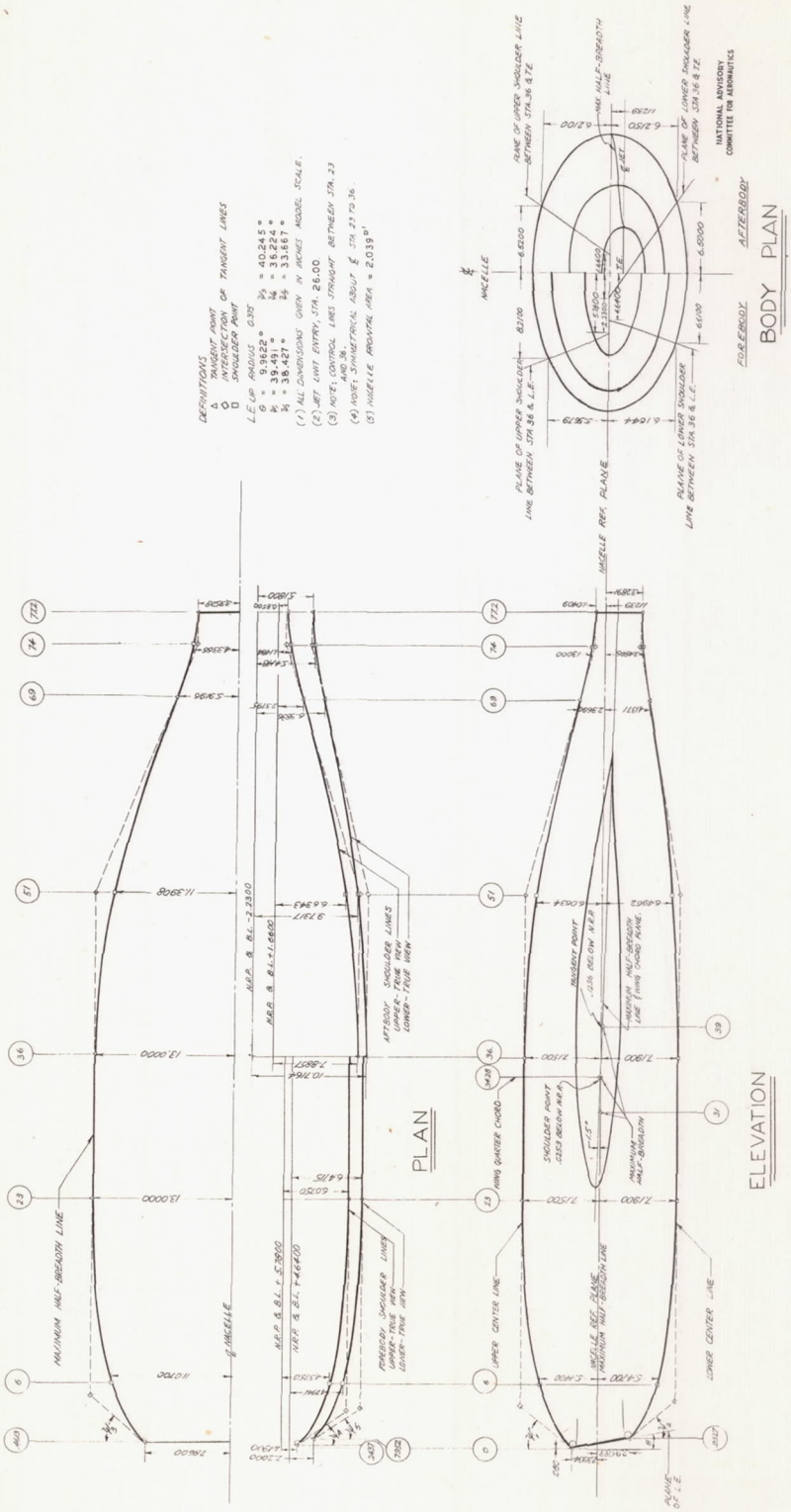

FIGURE 5.- CONTROL LINES FOR NACELLE B.

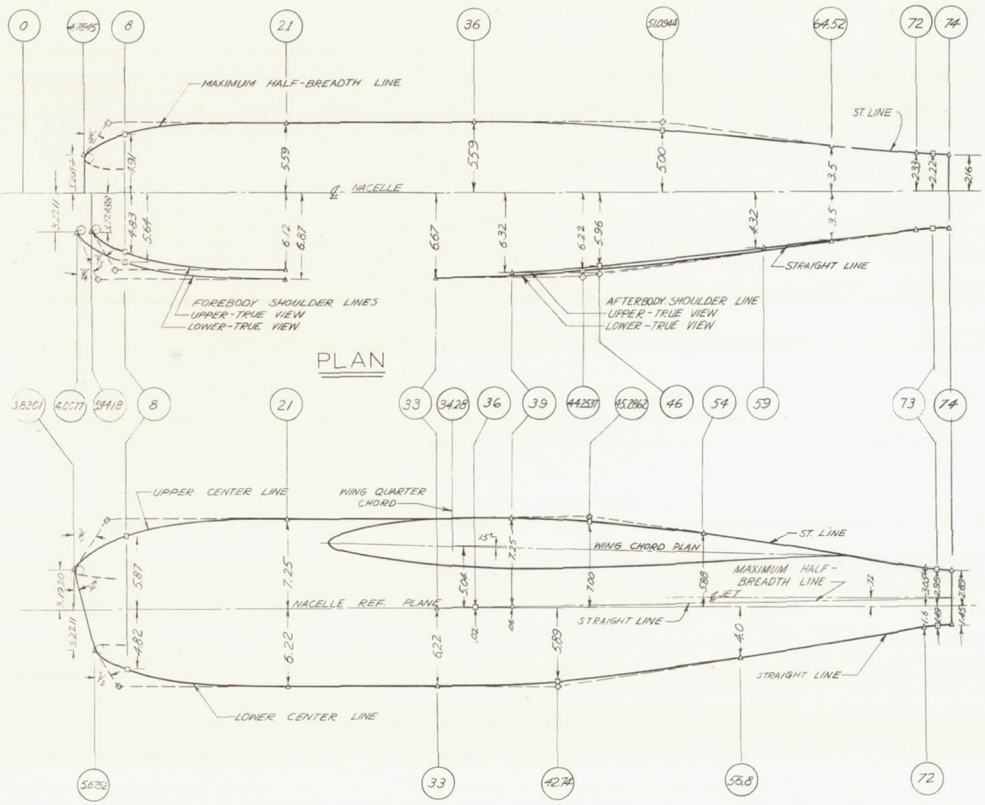

DEFINITIONS
- △ TANGENT POINT
- ◇ INTERSECTION OF TANGENT LINES.
- □ SHOULDER POINT

L.E. LIP RADIUS 0.375"

θ	= 16.375°	ψ_3	= 38°
ψ_1	= 25°	ψ_4	= 27.826°
ψ_2	= 30°	ψ_5	= 30.684°

(1) ALL DIMENSIONS GIVEN IN INCHES MODEL SCALE.

(2) JET UNIT ENTRY, STA. 23.35.

(3) NOTE: CONTROL LINES STRAIGHT BETWEEN STA. 21 TO 33, AND STA. 64.52 TO 72 FOR UPPER-TRUE VIEW, AND STA. 21 TO 33, AND STA. 59 TO 72 FOR LOWER-TRUE VIEW.

(4) NOTE: SYMMETRICAL ABOUT CENTER LINE STA. 72 TO 74.

(5) NACELLE FRONTAL AREA = 0.865 ft^2

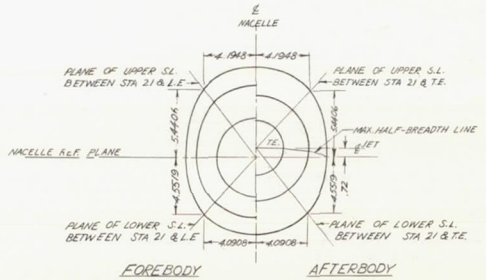

NATIONAL ADVISORY COMMITTEE FOR AERONAUTICS

BODY PLAN

FIGURE 6.- CONTROL LINES FOR NACELLE C.

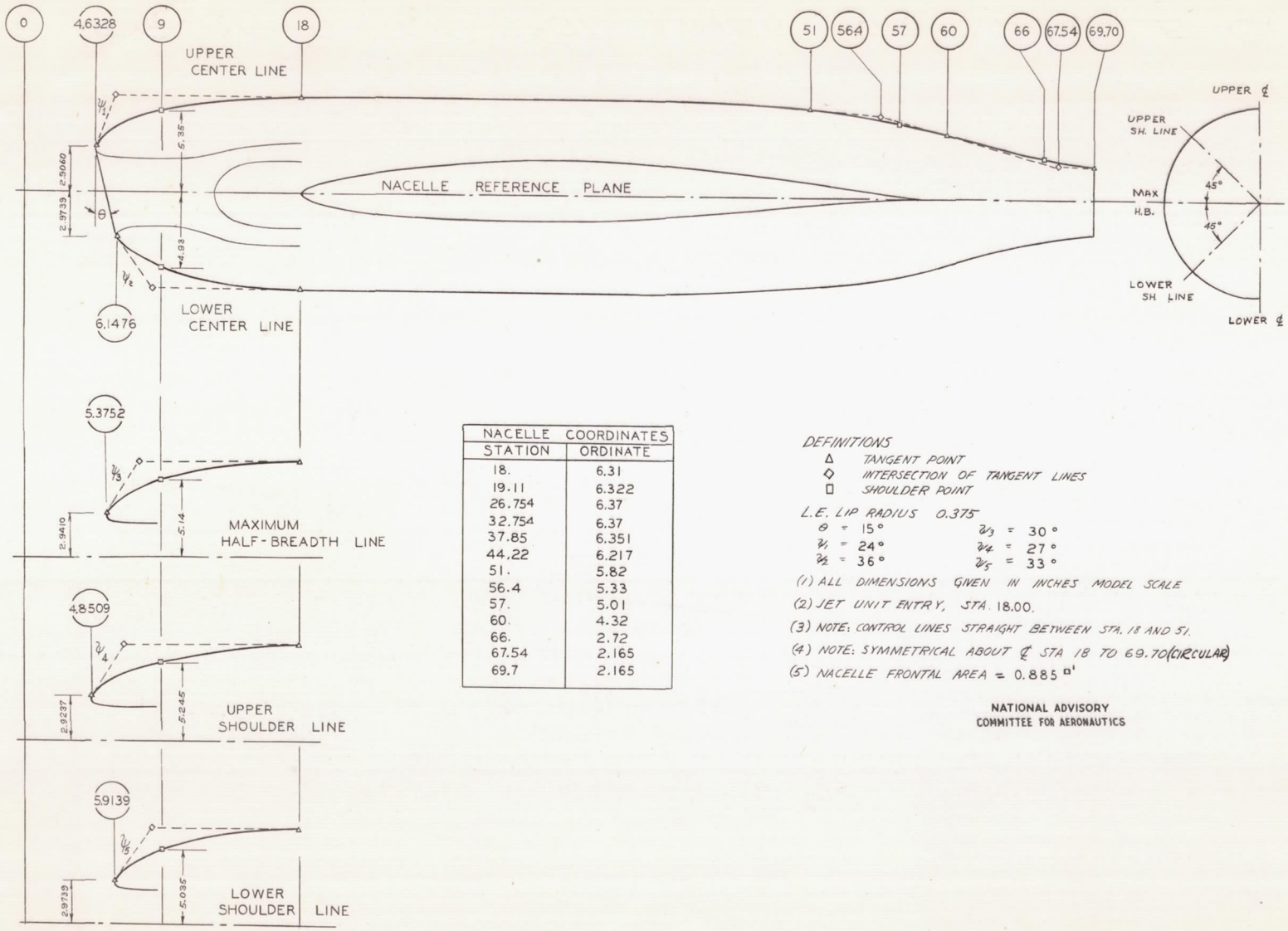

NACELLE STATION	COORDINATES ORDINATE
18.	6.31
19.11	6.322
26.754	6.37
32.754	6.37
37.85	6.351
44.22	6.217
51.	5.82
56.4	5.33
57.	5.01
60.	4.32
66.	2.72
67.54	2.165
69.7	2.165

DEFINITIONS

△ *TANGENT POINT*
◇ *INTERSECTION OF TANGENT LINES*
□ *SHOULDER POINT*

L.E. LIP RADIUS 0.375

$\theta = 15°$ $\quad \psi_3 = 30°$
$\psi_1 = 24°$ $\quad \psi_4 = 27°$
$\psi_2 = 36°$ $\quad \psi_5 = 33°$

(1) ALL DIMENSIONS GIVEN IN INCHES MODEL SCALE

(2) JET UNIT ENTRY, STA. 18.00.

(3) NOTE: CONTROL LINES STRAIGHT BETWEEN STA. 18 AND 51.

(4) NOTE: SYMMETRICAL ABOUT ℄ STA 18 TO 69.70 (CIRCULAR)

(5) NACELLE FRONTAL AREA = 0.885 ft^2

NATIONAL ADVISORY
COMMITTEE FOR AERONAUTICS

FIGURE 7.- CONTROL LINES FOR NACELLE D.

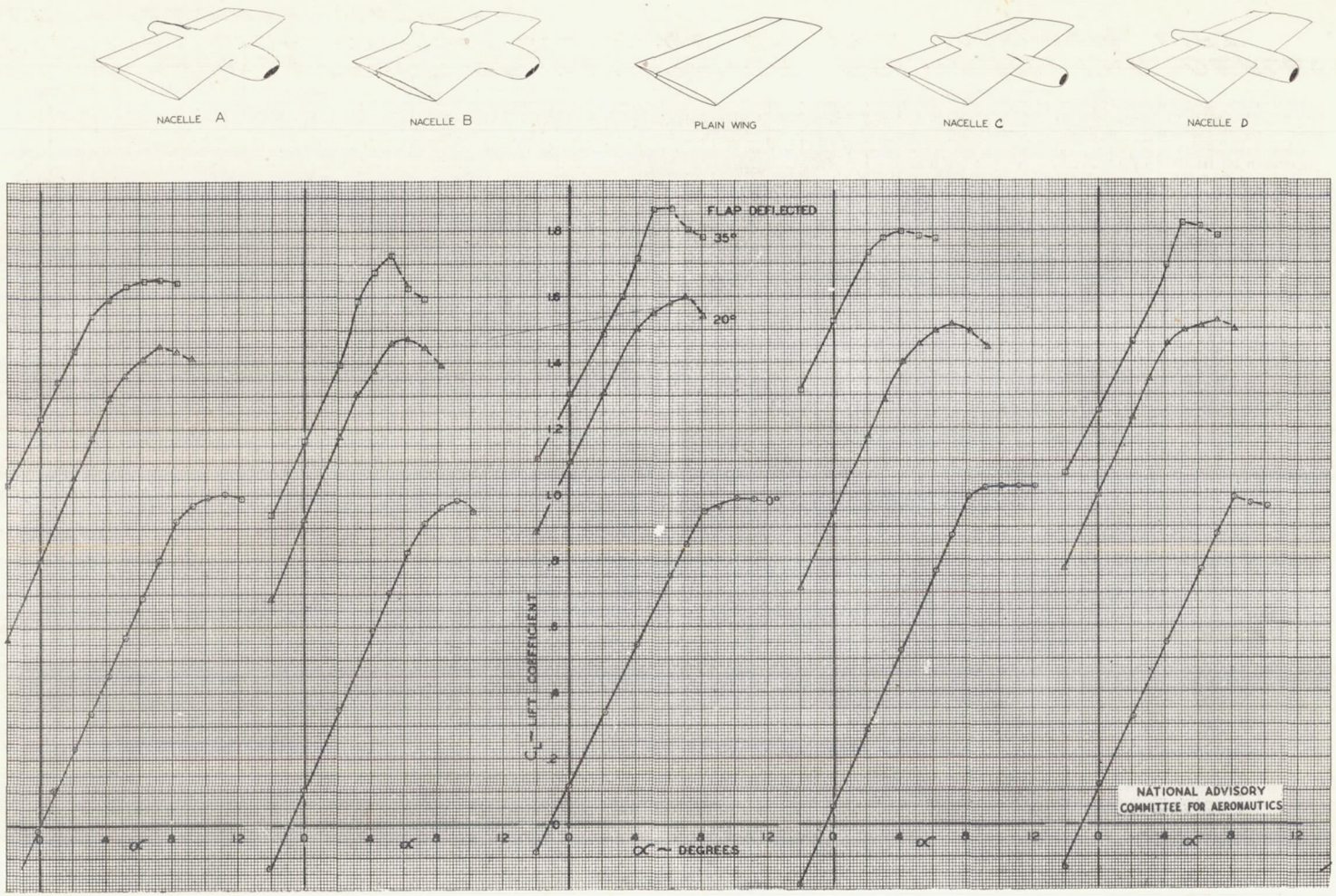

FIGURE 8.- THE LIFT CHARACTERISTICS OF THE NACA 65$_1$-210 WING AND NACELLES WITH 0.25C SLOTTED FLAP. INLET-VELOCITY RATIO = 0.

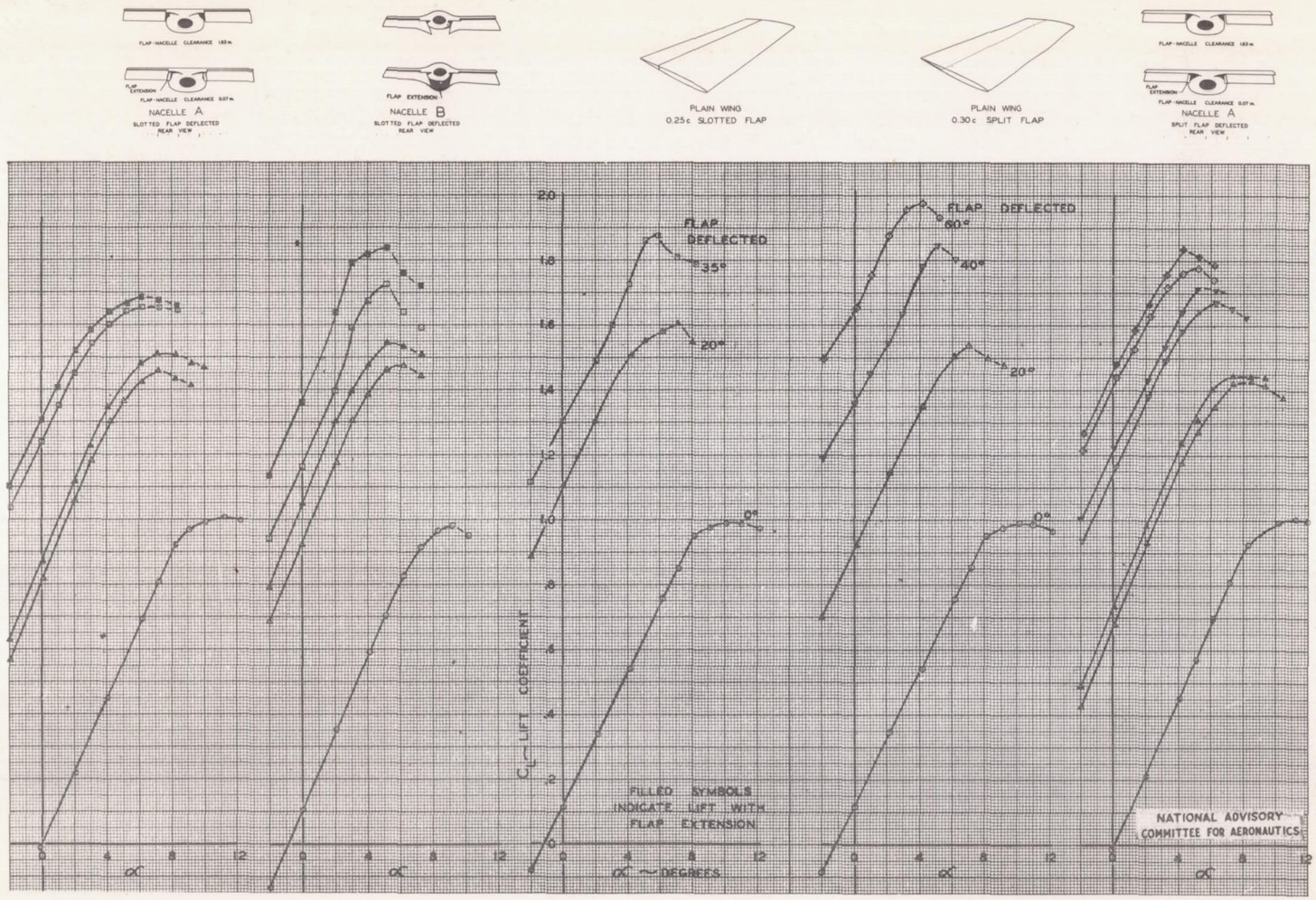

FIGURE 9.- THE EFFECT OF CLEARANCE BETWEEN THE DEFLECTED FLAP AND SIDE OF THE NACELLE ON THE MAXIMUM LIFT. INLET-VELOCITY RATIO = 0.

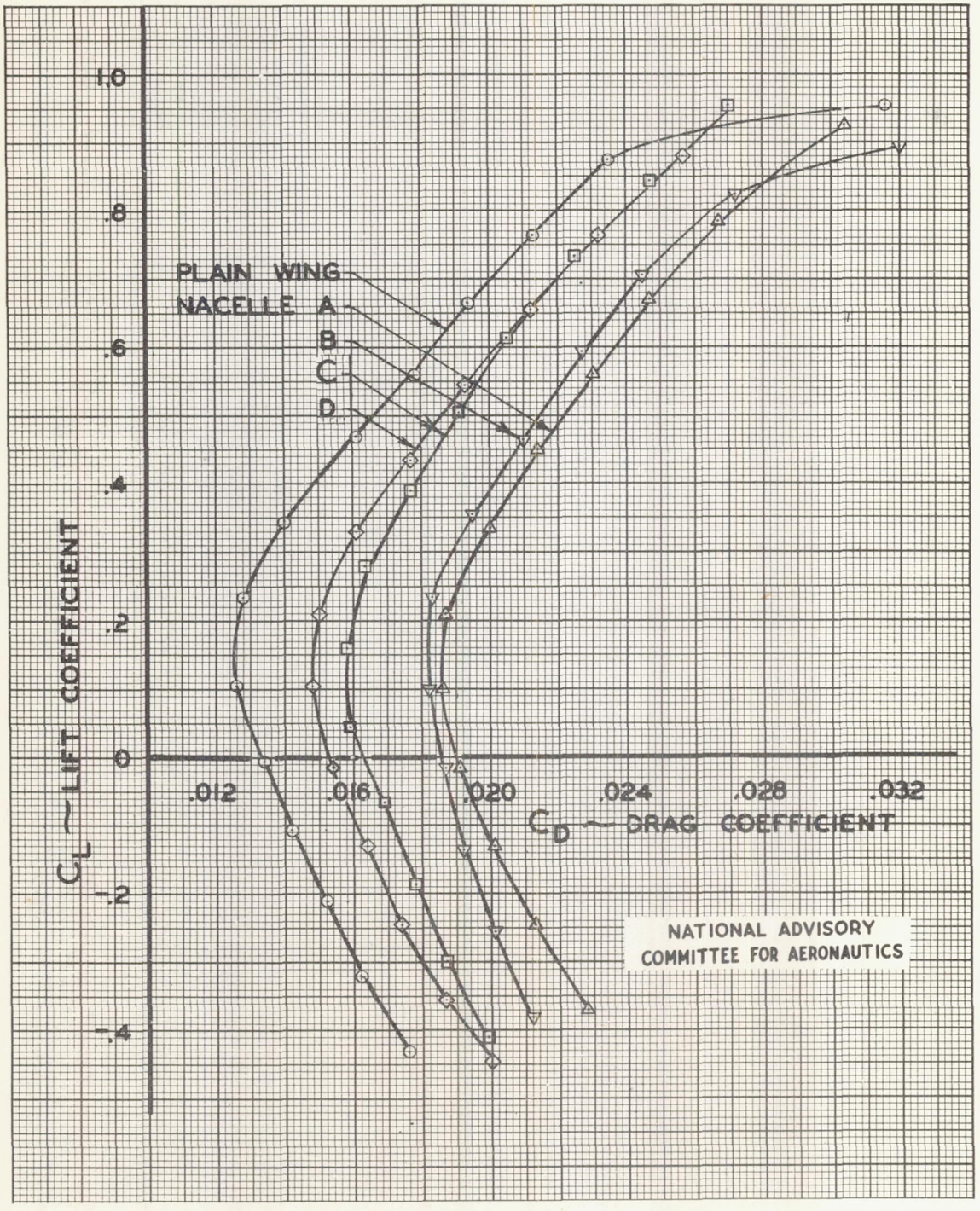

FIGURE 10.- THE TOTAL DRAG CHARACTERISTICS OF AN NACA 65,-210 WING AND NACELLES. INLET VELOCITY RATIO = 0.

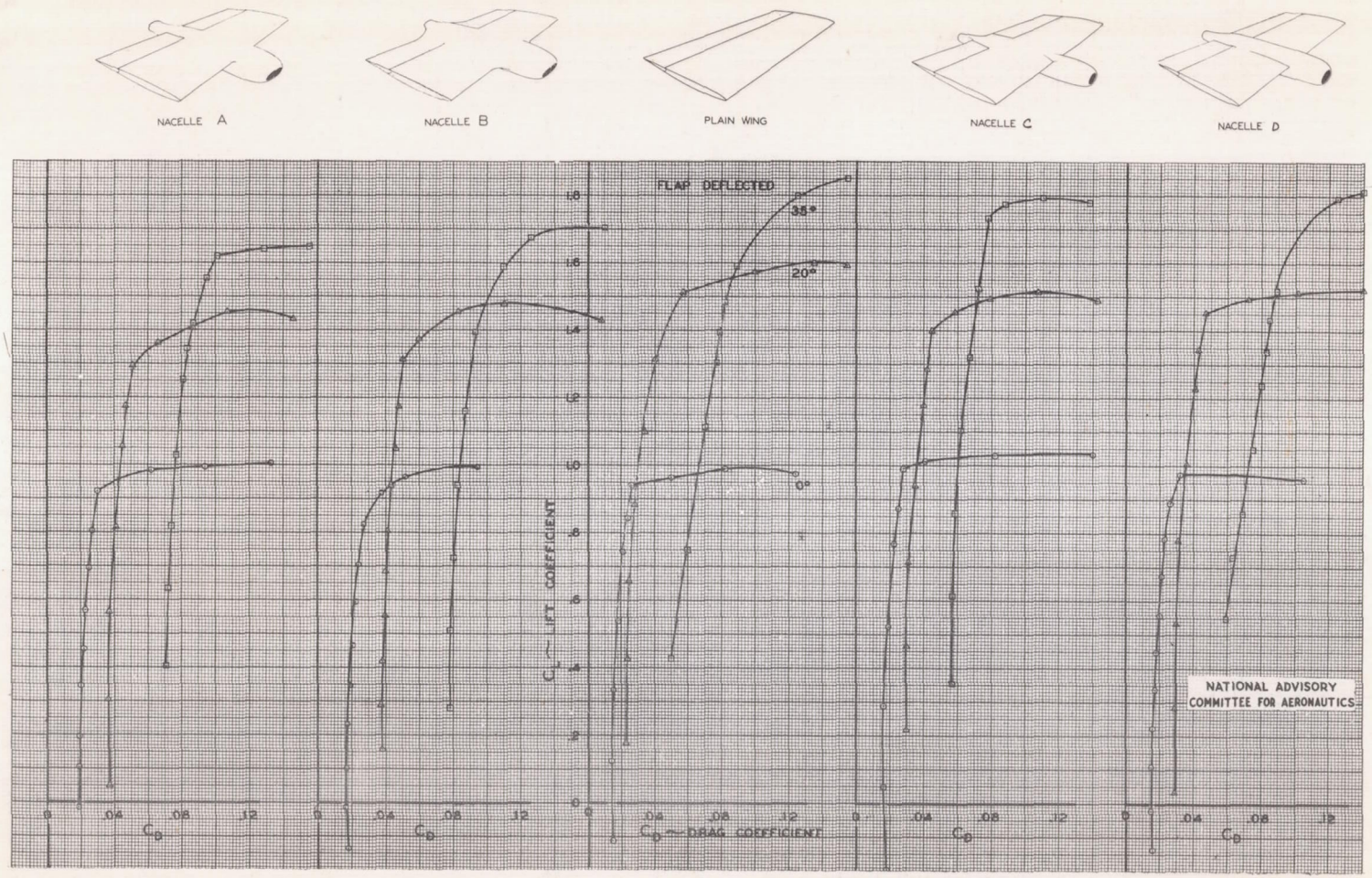

FIGURE 11.- THE DRAG CHARACTERISTICS OF THE NACA 65,-210 WING AND NACELLES WITH 0.25C SLOTTED FLAP. INLET-VELOCITY RATIO = 0.

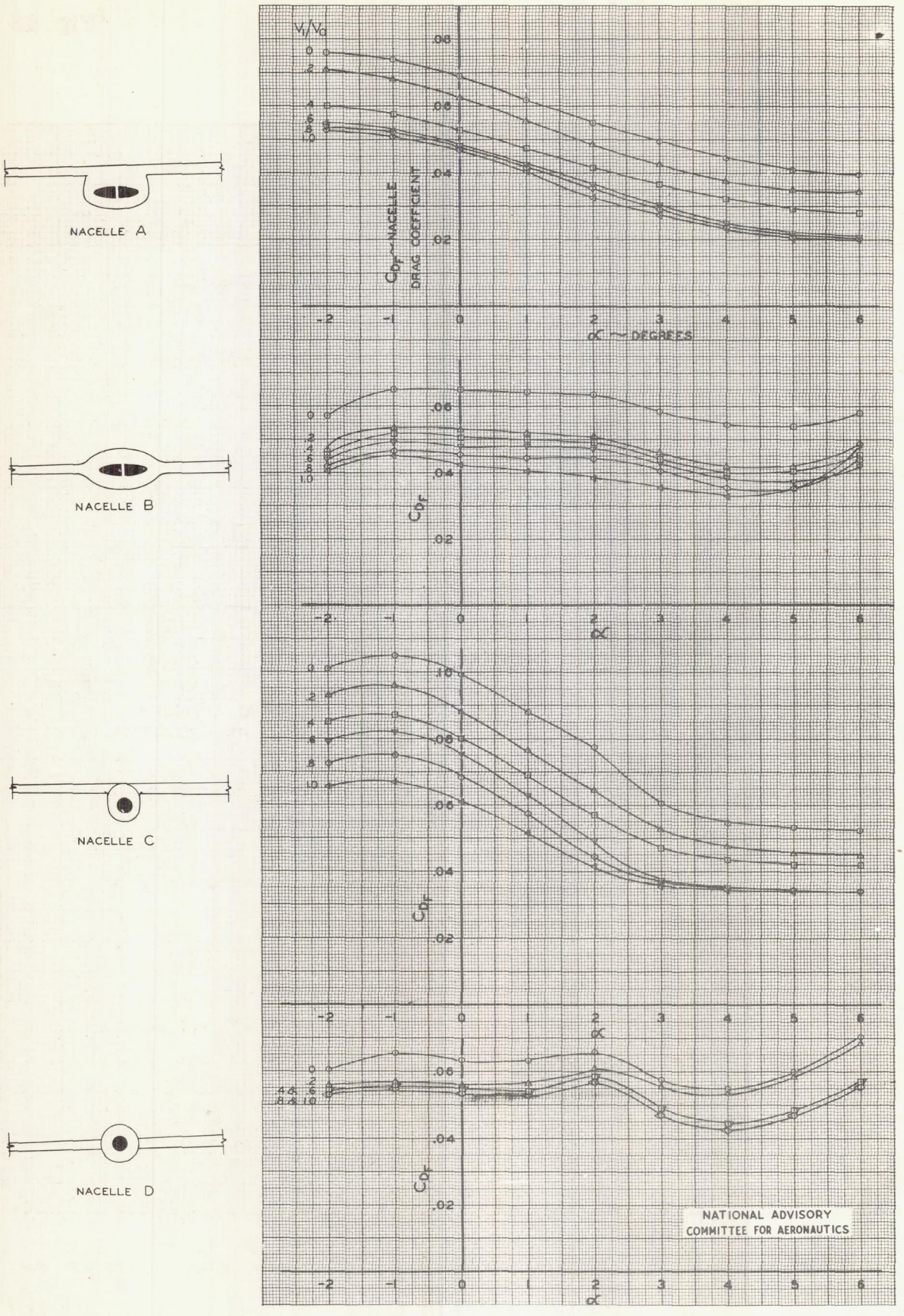

FIGURE 12.- VARIATION OF THE EXTERNAL DRAG COEFFICIENT OF THE NACELLES WITH ANGLE OF ATTACK.

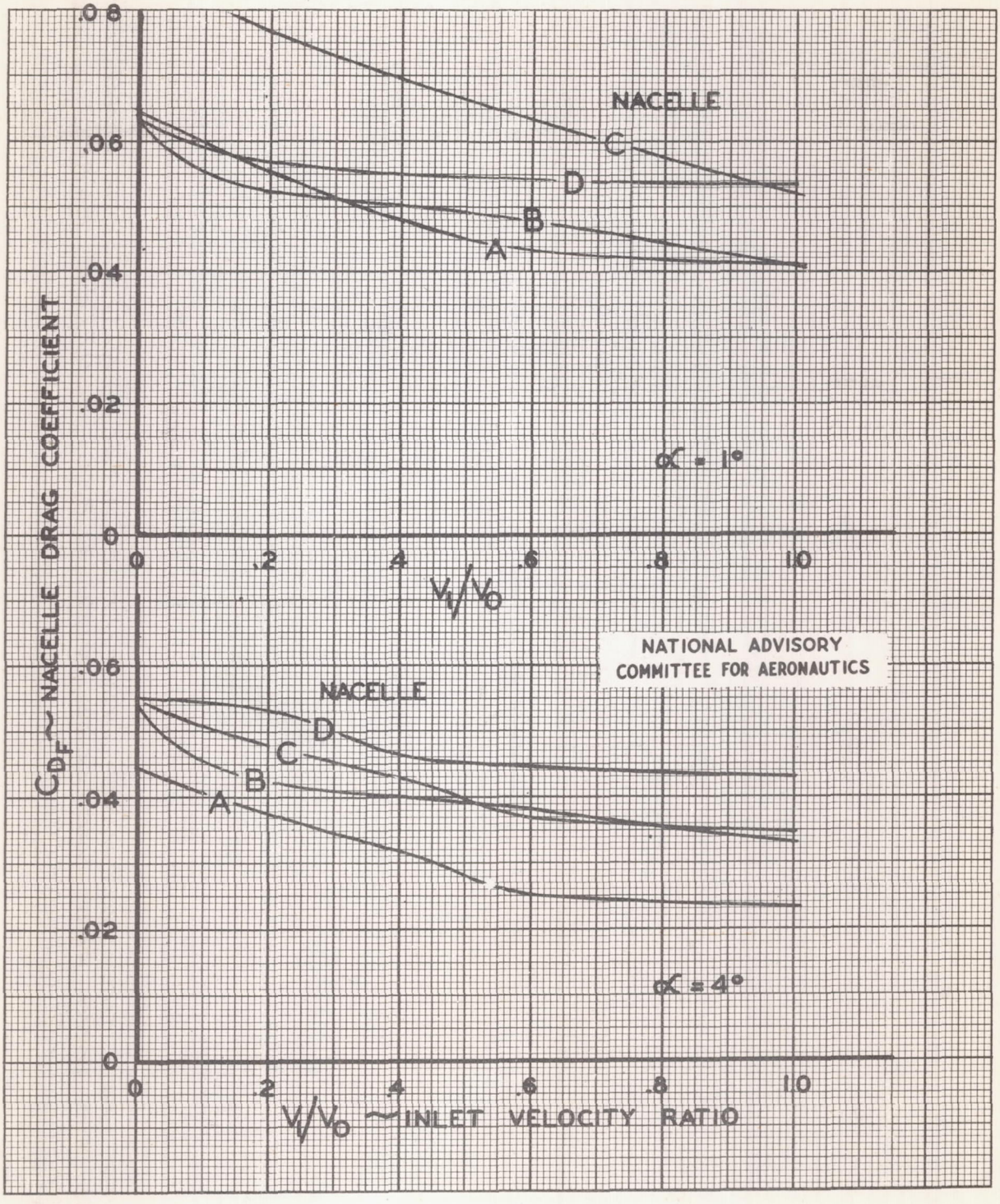

FIGURE 13.- VARIATION OF THE EXTERNAL DRAG COEFFICIENT OF THE NACELLES WITH INLET-VELOCITY RATIO.

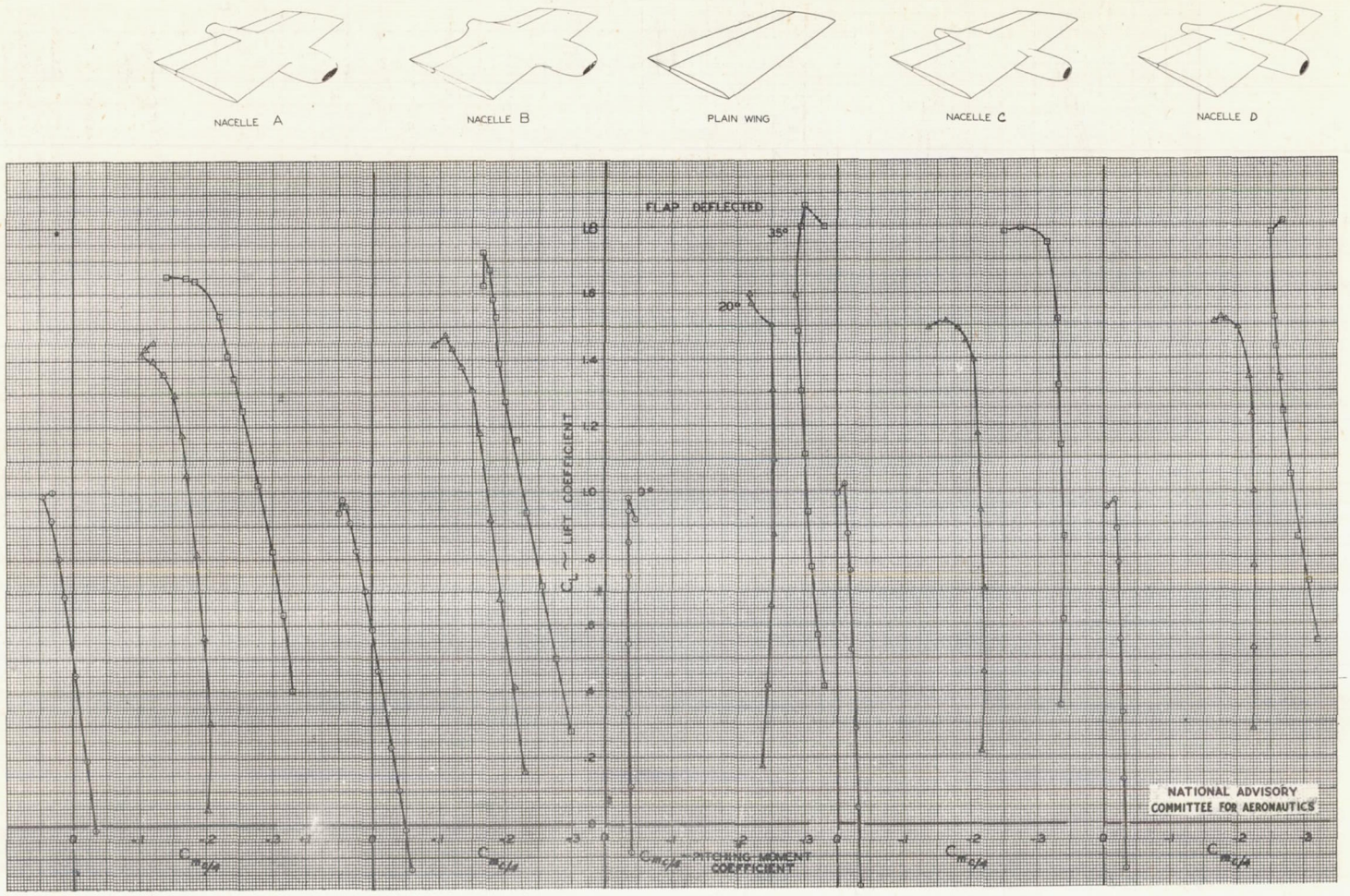

FIGURE 14.- THE PITCHING-MOMENT CHARACTERISTICS OF THE NACA 65$_1$-210 WING AND NACELLES WITH 0.25C SLOTTED FLAP. INLET-VELOCITY RATIO = 0.

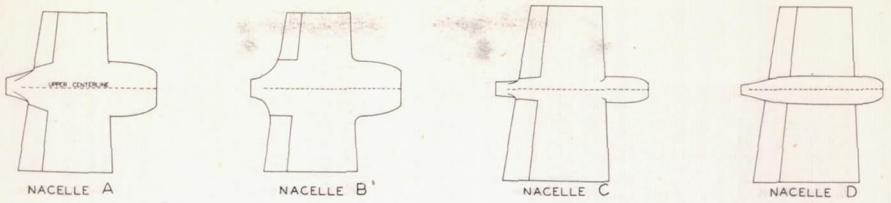

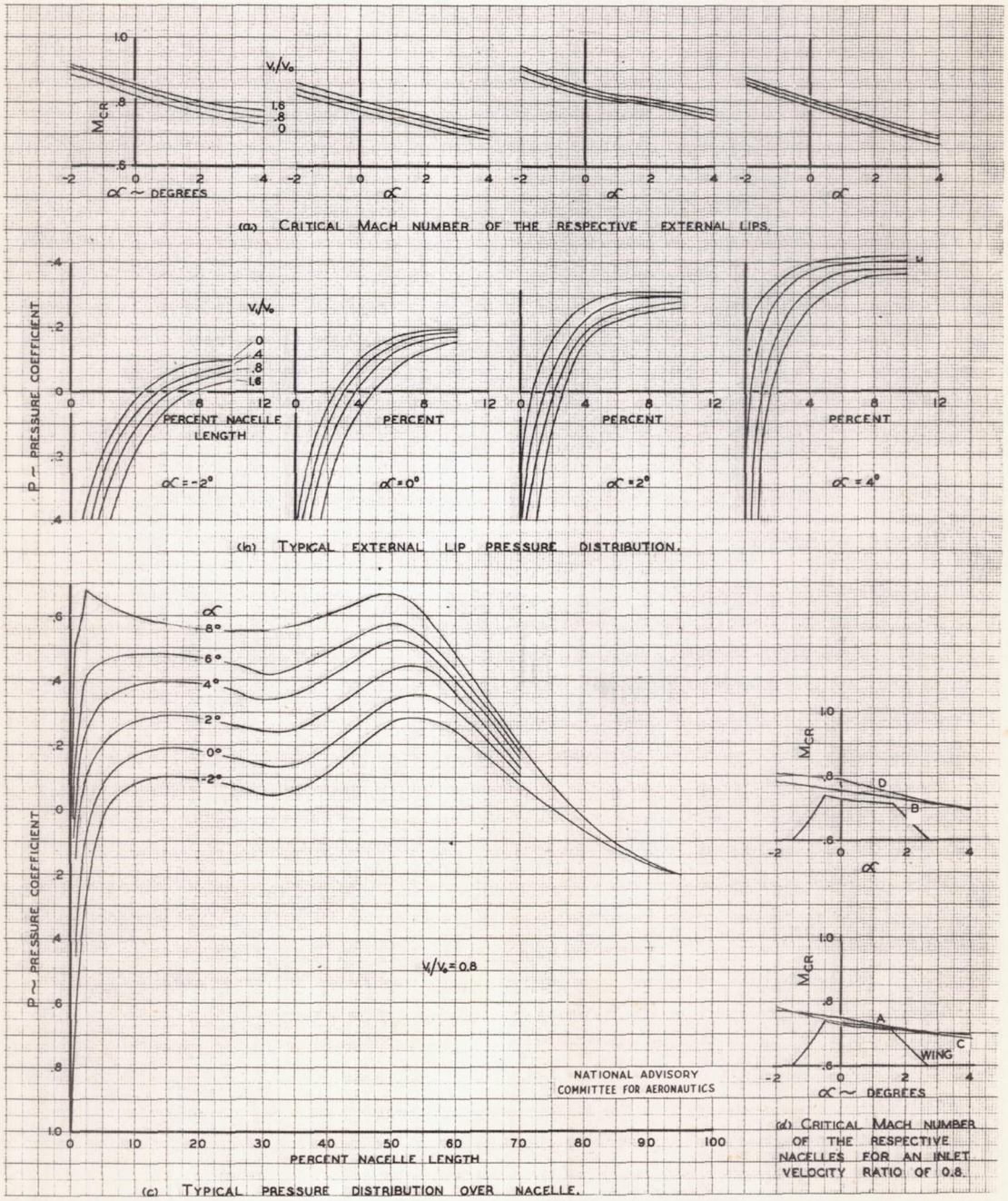

FIGURE 15.- PRESSURE-COEFFICIENT DISTRIBUTION AND CRITICAL MACH NUMBER VARIATION OVER THE UPPER CENTER LINE OF THE NACELLES.

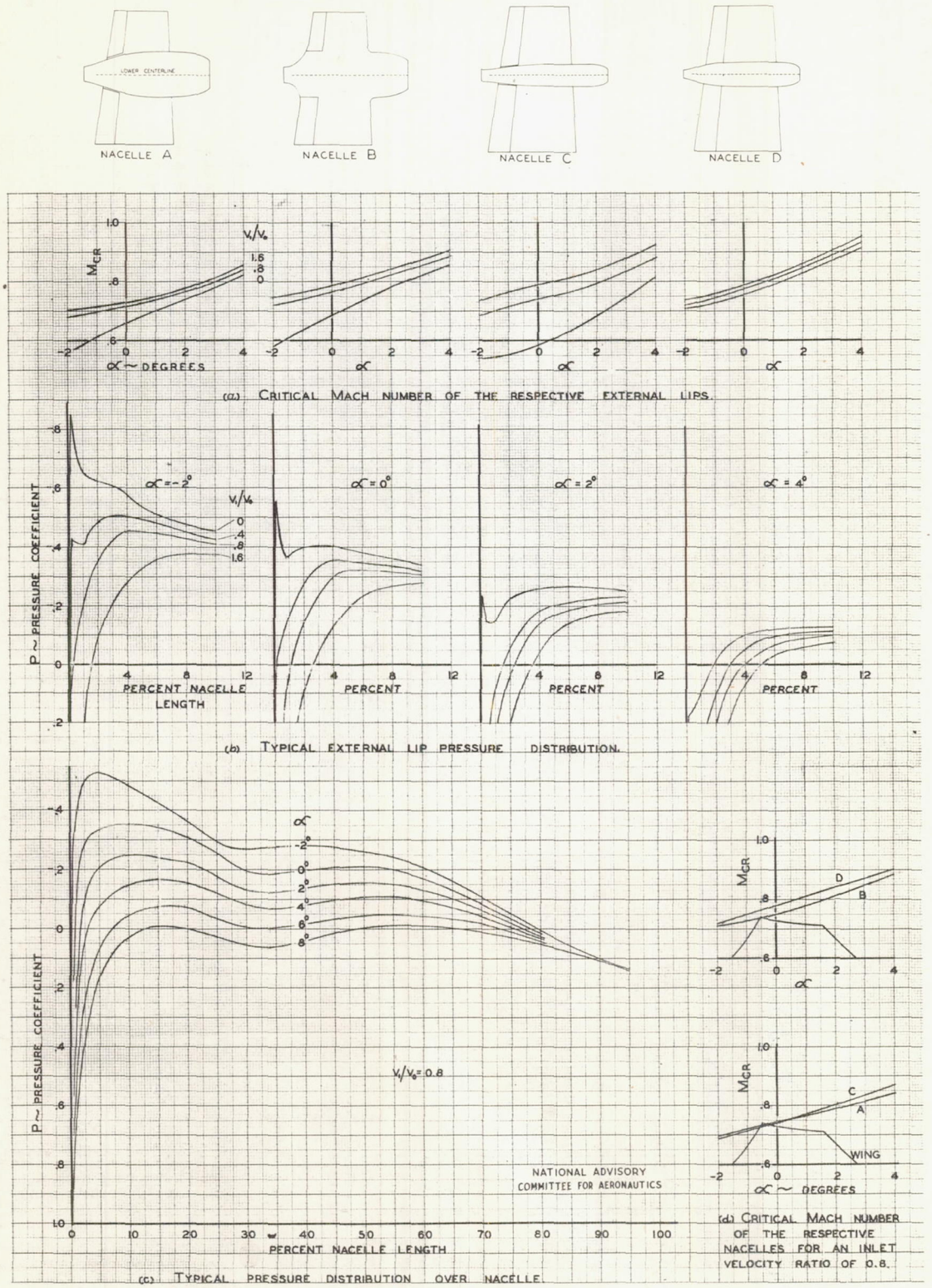

FIGURE 16.- PRESSURE-COEFFICIENT DISTRIBUTION AND CRITICAL MACH NUMBER VARIATION OVER THE LOWER CENTER LINE OF THE NACELLES.

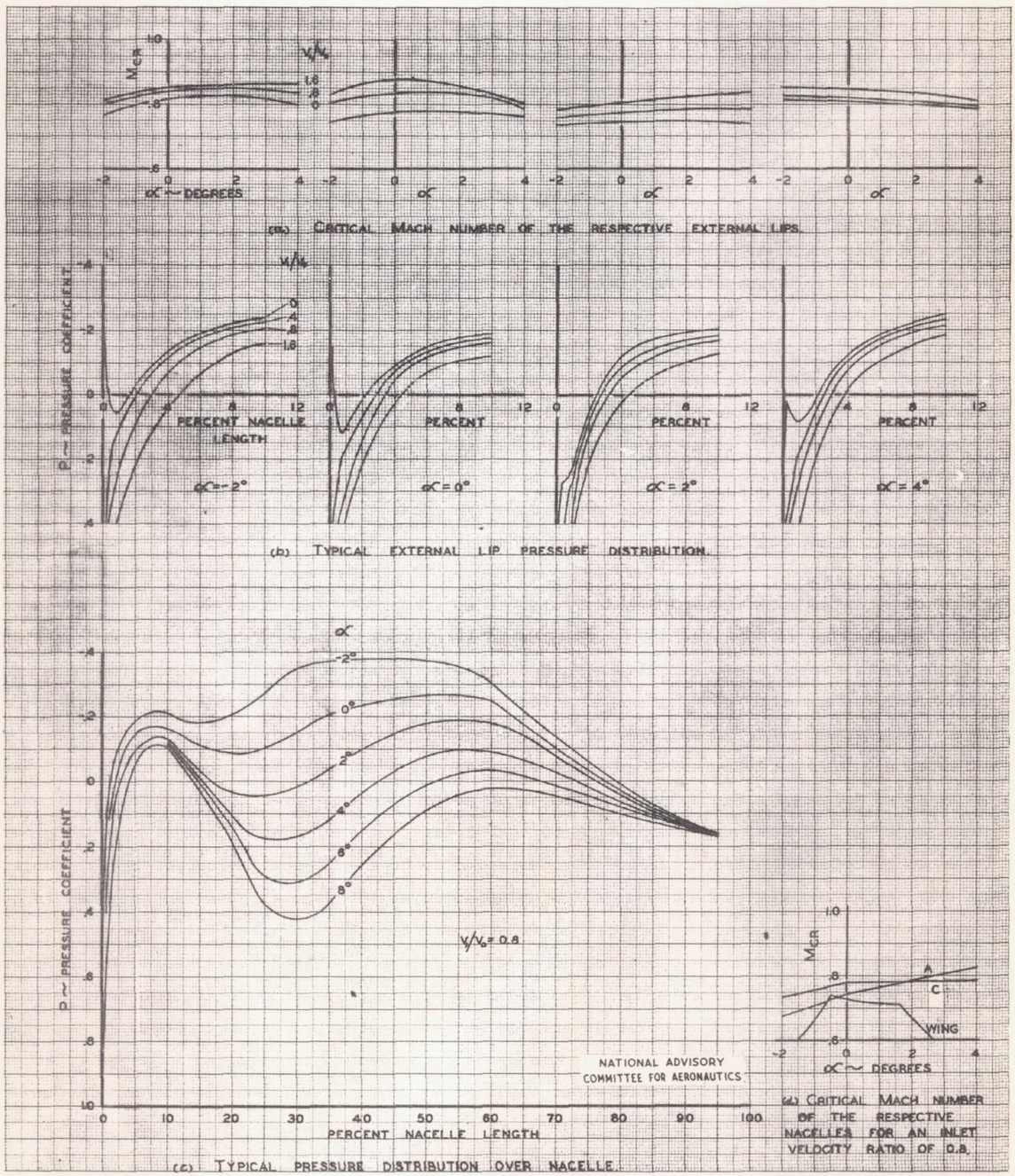

FIGURE 17.- PRESSURE-COEFFICIENT DISTRIBUTION AND CRITICAL MACH NUMBER VARIATION OVER THE MAXIMUM HALF-BREADTH LINE OF THE NACELLES.

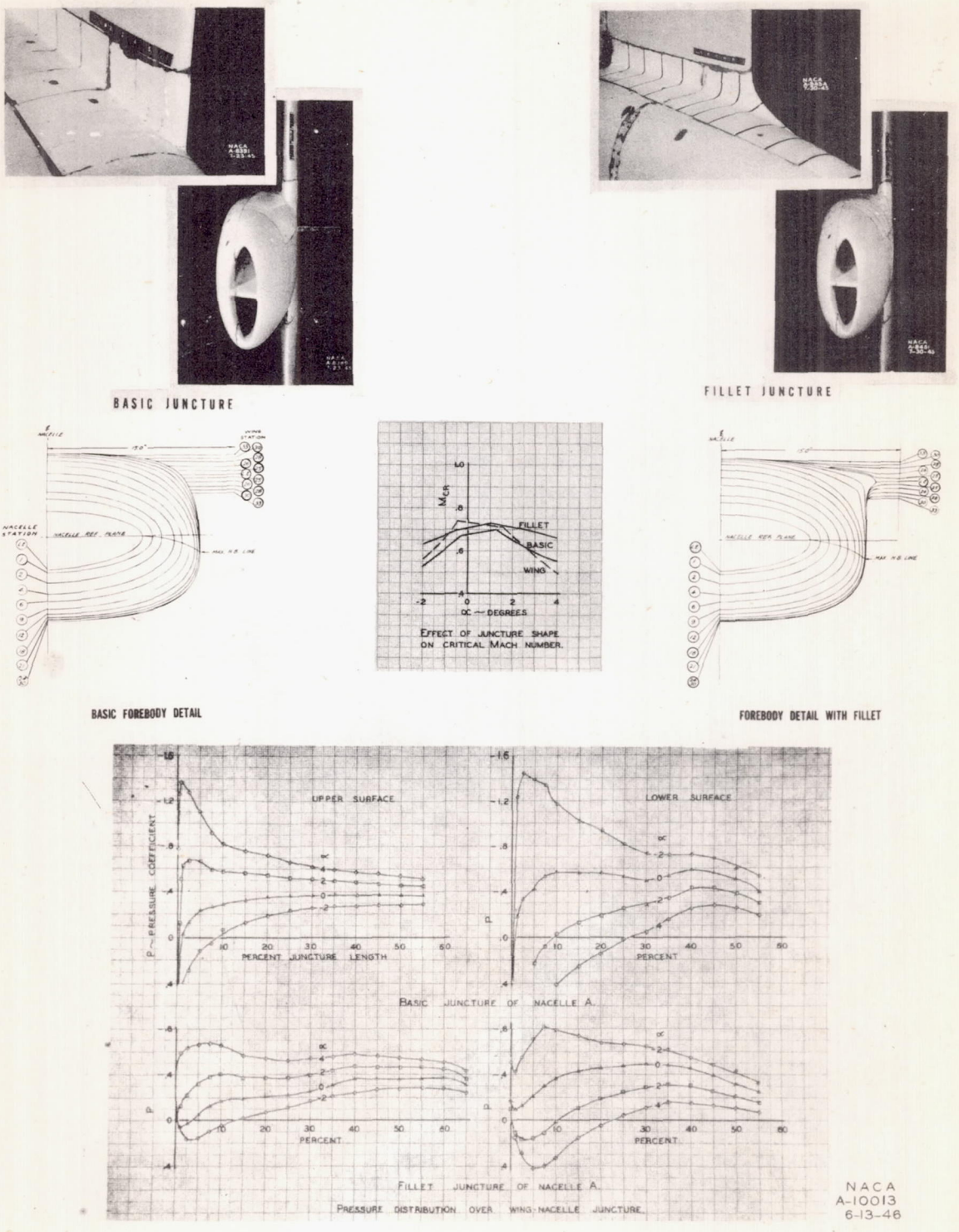

Figure 18.- Effect of fillets on the wing-nacelle juncture pressure distribution of nacelle A.

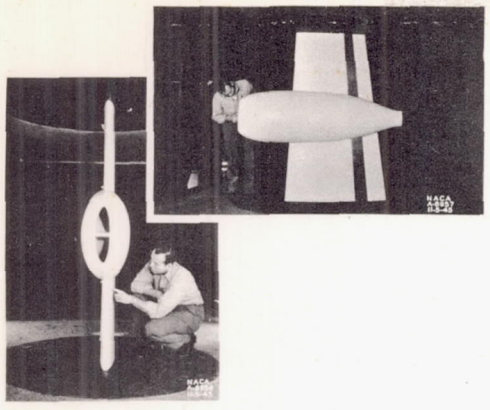

BASIC JUNCTURE

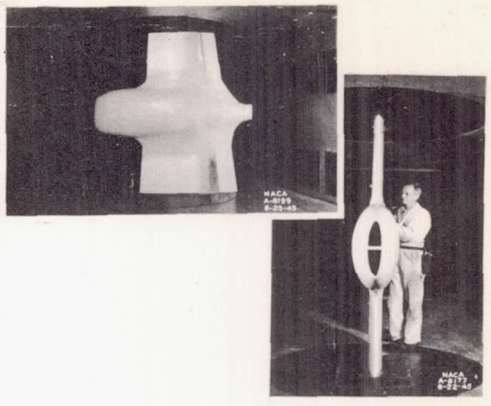

FILLET JUNCTURE

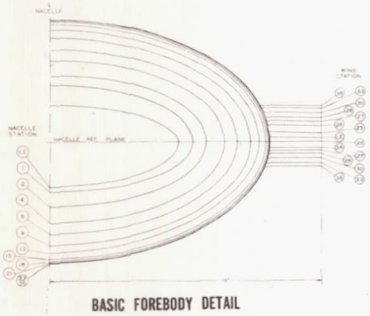

BASIC FOREBODY DETAIL

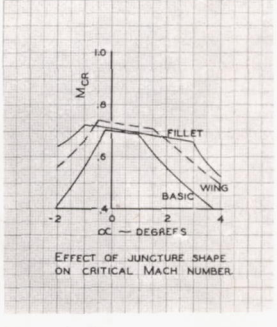

EFFECT OF JUNCTURE SHAPE ON CRITICAL MACH NUMBER

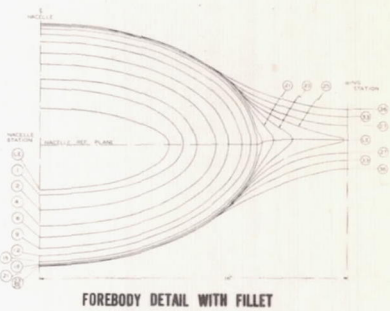

FOREBODY DETAIL WITH FILLET

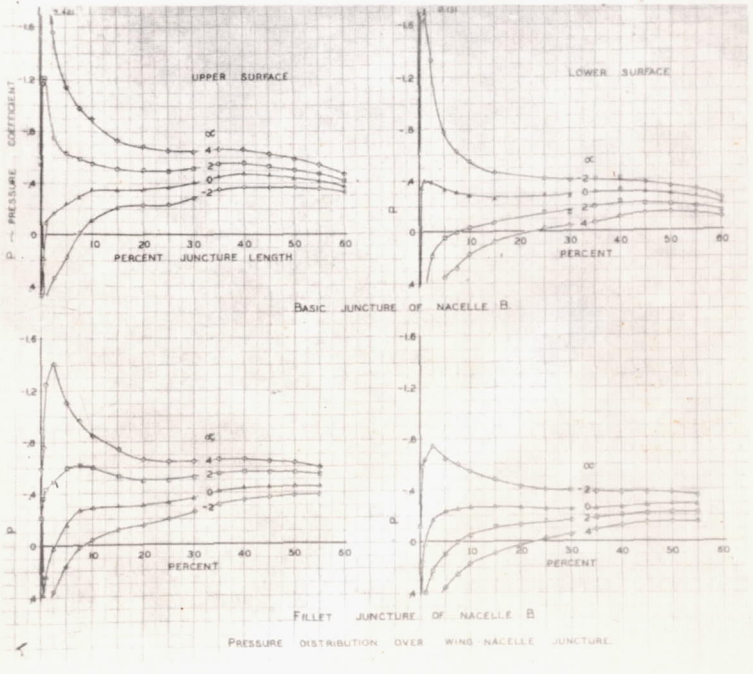

Figure 19.- Effect of fillets on the wing-nacelle juncture pressure distribution of nacelle B.

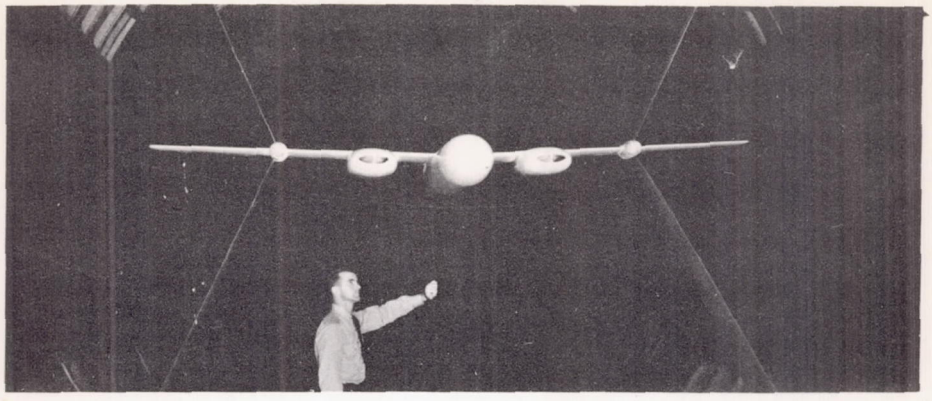

MODEL INSTALLATION IN 16-FOOT WIND TUNNEL

WING SECTION: NACA 65_1-210, $a = 1$

TAPER RATIO	2.5:1	SPAN	10.0 FT.
ASPECT RATIO	9	AREA	11.11 SQ. FT.
DIHEDRAL	3°	M.A.C.	1.180 FT.
NACELLE INCIDENCE	-1.5°	ROOT CHORD	1.587 FT.

PERCENT LINE STRAIGHT 25

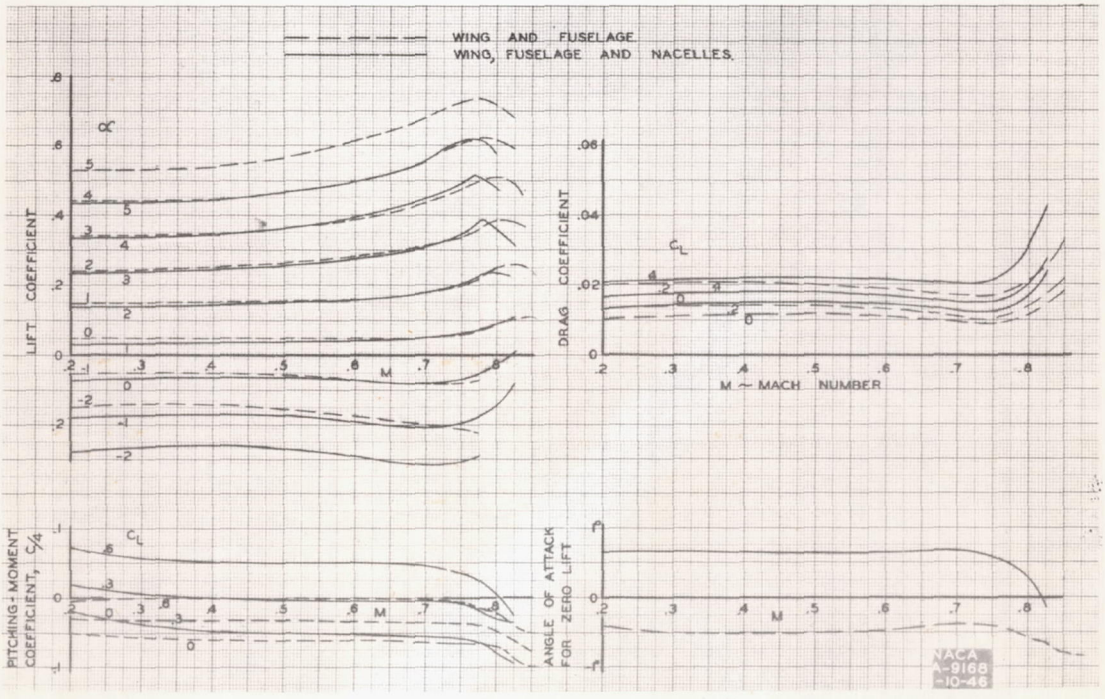

Figure 20.- High-speed characteristics of nacelle A from tests in the Ames 16-foot high-speed wind tunnel.

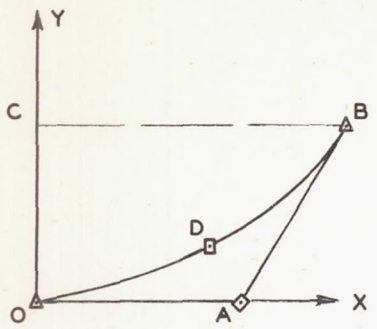

EQUATION: $Ax^2 + Bxy + Cy^2 + Dx + Ey + F = 0$

FUNCTION: $Y = \int(x)$

PARAMETER: $k = \frac{ec(a-d) - (a-b)e^2}{(cd - be)^2}$

CONSTANTS:

$P = \frac{2bck - c}{2(a - b + b^2k)}$

$Q = \frac{ac}{2(a - b + b^2k)}$

$R = \frac{c^2 - 4ac^2k}{4(a - b + b^2k)^2}$

$S = 2PQ$

$T = Q^2$

CONTROL POINTS

O: (0, 0)
A: (a, 0)
B: (b, c)
C: (0, c)
D: (d, e)

SOLUTION:

$$Y = Px + Q - \sqrt{Rx^2 + Sx + T}$$

△ TANGENT POINT
⊡ SHOULDER POINT
◇ INTERSECTION OF TANGENT LINES

NATIONAL ADVISORY COMMITTEE FOR AERONAUTICS

(a) FORMULAE FOR EVALUATING A CONIC EQUATION.

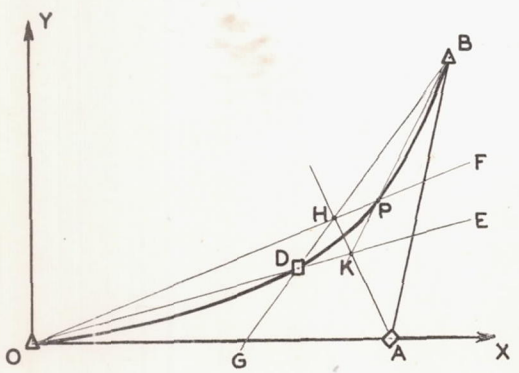

THE TANGENTS TO THE REQUIRED CURVE AT THE POINTS OF CONTACT O AND B ARE OA AND AB. THE GIVEN SHOULDER POINT THROUGH WHICH THE CONIC CURVE ODB MUST PASS IS D.

THE GRAPHICAL CONSTRUCTION TO LOCATE ANY POINT P ON THE CONIC CURVE IS AS FOLLOWS:

1. DRAW LINES OE AND BG THROUGH D,
2. DRAW RADIAL LINE OF TO INTERSECT BG AT H,
3. DRAW AH TO INTERSECT OE AT K,
4. DRAW BK, A LINE WHICH WILL INTERSECT HF AT THE DESIRED POINT P.

OTHER POINTS ON THE CURVE ARE OBTAINED BY DRAWING OTHER LINES THROUGH O AND B.

(b) GRAPHICAL CONSTRUCTION TECHNIQUE FOR THE GENERAL CONIC.

FIGURE 21. - NACELLE LOFTING METHOD.